Numerology-Persistence Coupling Performance in 5G NR-V2X Sidelink Communication

Alexey Rolich*, Mert Yildiz*, Asmad Bin Abdul Razzaque*, Ion Turcanu†, Alexey Vinel‡, Andrea Baiocchi*
*University of Rome Sapienza, Italy
†Luxembourg Institute of Science and Technology (LIST), Luxembourg
‡Karlsruhe Institute of Technology (KIT), Karlsruhe, Germany
alexey.rolich@uniroma1.it mert.yildiz@uniroma1.it asmadbin.razzaque@uniroma1.it
ion.turcanu@list.lu alexey.vinel@kit.edu andrea.baiocchi@uniroma1.it

***Abstract*—The impact of numerology selection on 5G New Radio (NR) Vehicle-to-Everything (V2X) sidelink communications, particularly its coupling with persistence mechanisms like Semi-Persistent Scheduling (SPS), has been insufficiently explored. This paper investigates how numerology-persistence coupling affects Age of Information (AoI) and system performance in sub-6 GHz NR-V2X deployments. Our analysis shows that at low-to-moderate vehicle densities, the performance differences across numerologies are minimal. However, under high channel load, numerology selection plays a key role in performance, with higher numerologies leading to increased collisions and reduced resource availability, which degrade performance. The results emphasize the importance of evaluating numerology in a cross-layer context (PHY and MAC layers), where lower numerologies tend to offer better performance, particularly in high-density environments, by providing a larger resource pool and reducing collisions.**

***Index Terms*—5G NR-V2X Sidelink, Numerology, Persistence, Age-of-Information**

I. Introduction

Vehicle-to-Everything (V2X) communication is a core enabler of modern Intelligent Transportation Systems (ITS), supporting real-time information exchange among vehicles, infrastructure, and Vulnerable Road Users (VRUs). It underpins cooperative awareness and low-latency decision-making for safety-critical functions such as collision avoidance, cooperative adaptive cruise control, and platooning.

In 5G New Radio (NR), numerology (μ) defines the Orthogonal Frequency-Division Multiple Access (OFDM) Sub-Carrier Spacing (SCS) (Δf) and Cyclic Prefix (CP) configuration [1]. Unlike Long-Term Evolution (LTE)'s fixed 15 kHz spacing, NR supports scalable SCS values from 15 kHz up to 960 kHz [2], selected according to carrier frequency and service requirements [3]. This flexibility is essential across Frequency Range 1 (FR1) (sub-6 GHz) and Frequency Range 2 (FR2) (mmWave), where a single numerology cannot jointly satisfy latency, robustness, and spectral-efficiency constraints. In V2X, larger SCS shortens slot duration and improves Doppler tolerance, which benefits high mobility and mmWave operation, whereas smaller SCS improves spectral efficiency and allows longer CP, increasing resilience to delay spread. These benefits come with trade-offs: small SCS is more sensitive to mobility-induced loss of orthogonality and can increase Inter-Symbol Interference (ISI) in multipath conditions, while large SCS reduces frequency-domain granularity and may waste spectrum in narrowband deployments [4, 5].

Numerology also impacts sidelink resource allocation. In NR-V2X Mode 2, User Equipments (UEs) autonomously select resources – one or more Sub-Channels (SCs) – from a resource pool, enabling operation without coverage; under coverage, the gNB or eNB can (pre-)configure the pool to improve efficiency. 5G NR-V2X sidelink supports Dynamic Scheduling (DS) and Semi-Persistent Scheduling (SPS) for resource allocation. DS selects resources per Transport Block (TB) (with reservations only for retransmissions), whereas SPS reserves resources for repeated transmissions and is suited to periodic traffic such as Cooperative Awareness Message (CAM) and Basic Safety Message (BSM). With SPS, UEs sense the channel, select a SC, and persistently reuse it at a Resource Reservation Interval (RRI) governed by the Reselection Counter (RC) and the probability of persistence (P). While persistence reduces overhead, it can extend collisions under, producing bursty losses consistent with Gilbert-Elliott-like behavior [6]. Further SPS details are in [3, 7].

A key open issue is how numerology interacts with SPS persistence in sidelink: numerology changes both PHY behavior and slot duration, and it reshapes the MAC-layer resource pool, thereby affecting collision dynamics and resource availability. This paper investigates numerology-persistence coupling in 5G NR-V2X sidelink (mode 2) across scenarios, showing that numerology should be selected using metrics beyond Packet Reception Ratio (PRR) and delay, including collision duration, disconnection behavior, and timeliness – especially Age of Information (AoI) – to ensure safe and reliable vehicular communications.

The main contributions of this paper are as follows:

- To the best of our knowledge, this work is the first to investigate the impact of numerology on AoI. Under low-to-moderate channel load, the numerology-persistence coupling exhibits non-monotonic behavior, with the minimum AoI achieved under weak or moderate persistence (according to the adopted classification in [6]). Under high channel load, non-monotonic behavior is also observed; however, DS (i.e., no persistence) consistently outperforms all persistence-based configurations across all numerologies.

IEEE 103rd Vehicular Technology Conference (VTC2026-Spring)

- Our analysis reveals that, for FR1, at low-to-moderate channel load, the quantitative performance difference across numerology-persistence coupling is negligible. However, in high channel load scenarios, increasing the SCS can degrade sidelink performance due to reduced resource availability and increased collision effects, in contrast to the findings in [8, 9].

The remainder of this paper is organized as follows. Section II reviews related work on numerology in 5G networks, with particular emphasis on vehicular communications. Section III presents the system model and describes the simulation environment. Section IV defines the evaluation metrics, analyzes the simulation results, and discusses the impact of numerology-persistence coupling on system performance. Finally, Section V concludes the paper.

II. Background and Related Works

To date, research on the impact of numerology on communication performance remains limited. Existing studies, conducted across various scenarios, report conflicting results, challenging the expectation that higher numerologies necessarily improve communication performance.

The study by Segura et al. [10] investigates the impact of numerology selection in 5G networks for industrial applications, particularly for Ultra Reliable and Low Latency Communications (URLCC). The authors find that higher numerologies do not always reduce delays, especially under Non-Line-of-Sight (NLOS) conditions or with larger packet sizes. Hossain and Ansari [11] explore the effect of numerology schemes on a sliced time-division duplex radio access network using sub-6 GHz and mmWave bands. They demonstrate that lower numerologies benefit high-throughput applications, while higher numerologies reduce power consumption and latency. In [12], the impact of 5G NR numerologies on latency in realistic TCP and UDP scenarios is examined. While TCP performance improves with higher numerologies, uplink UDP latency may increase due to processing delays and signaling overhead. The study suggests that numerology selection should account for traffic patterns and delays. Flores de Valgas et al. [5] analyze 5G NR numerologies across various deployment scenarios, with a focus on interference and device mobility. They conclude that numerology selection depends not only on the frequency band but also on the deployment scenario and UE speed. Their findings indicate that while increasing subcarrier spacing reduces Inter-Carrier Interference (ICI), it may increase ISI due to a smaller CP.

Several studies have investigated the impact of numerologies in V2X communications. Wang et al. [13] compare LTE C-V2X and 5G NR-V2X, focusing on scalable numerologies and their effects on PHY performance. The results suggest that 5G NR benefits from flexible numerologies, particularly at higher SCS values. For 15 kHz, LTE and 5G NR perform similarly, but at 30 kHz, 5G NR shows significant improvements. In [14], the same authors further investigate 5G NR-V2X performance, focusing on flexible numerology, variable SCS, and retransmission schemes. They find that while flexible numerologies enhance frequency domain utilization, their impact on PRR is minimal. In contrast, retransmission schemes with adaptive resource allocation significantly improve reliability, achieving PRR above 90 %. Soni et al. [15] propose an adaptive system for V2X communications that meets reliability and latency requirements under varying mobility and channel conditions. The system dynamically adjusts transmission numerology, improving robustness against Doppler and multipath effects. Their proposed numerology selection algorithm, which adapts to channel conditions like Signal-to-Noise Ratio (SNR) and Doppler spread, outperforms traditional link adaptation, offering improved performance in mobile scenarios. Khabaz et al. [4] report that higher 5G NR numerologies improve throughput and reduce latency for both safety and infotainment V2X applications. However, they note that the choice of the optimal numerology depends on propagation channel conditions, vehicle speed, and interference issues such as ICI and ISI. Therefore, selecting the appropriate numerology involves balancing the stringent requirements of V2X applications with the physical layer challenges.

Two studies [8, 9] explore the performance of 5G NR-V2X in autonomous sidelink mode, focusing on flexible numerology. Campolo et al. [8] compare C-V2X with NR-based solutions, which use scalable SCS and shorter Transmission Time Intervals (TTIs) to improve reliability and timeliness of CAMs. The study finds that reducing TTI and increasing numerology enhances PRR and reduces Packet Inter-Reception Delay (PIR). However, the fixed persistence probability value of 0.8 used in the study may "freeze" the communication channel in terms of resource allocation [6, 7, 16], negatively affecting sidelink communication performance. Ali et al. [9] show that higher numerologies improve performance by reducing simultaneous transmissions, thus lowering PIR. They demonstrate that higher numerologies benefit both sensing-based and random selection procedures, although random selection still lags behind sensing-based methods in terms of performance. Notably, they use a persistence probability of 0.

Currently, there is a gap in research regarding the impact of numerology in V2X communications, especially sidelink, which is highly sensitive to performance factors such as collisions and number of available resources. Numerology affects not only physical layer aspects and slot duration but also the channel configuration at the MAC layer, making it a key aspect to study in relation to sidelink and persistence. Preliminary analysis of the standard [17] indicates that, in FR1, for most configurations where all numerologies are applicable, the lowest numerology ($\mu = 0$) provides more resources within a single RRI than $\mu = 1$ and $\mu = 2$, leading to better resource utilization.

To address this gap, this paper investigates the coupling between different numerologies and the full range of SPS persistence levels. Unlike prior works that use fixed persistence, we analyze how these parameters jointly impact the timeliness of information – quantified through AoI – and collision dynamics under varying channel loads. Our study highlights that the selection of numerology must be informed by its impact on the MAC-layer resource pool, particularly in high-density

Table I
10 MHz CHANNEL CONFIGURATION FOR DIFFERENT NUMEROLOGIES.

μ	Δf **kHz**	**Total RBs**	N_{RB}	N_{SC}	S_{TBS} bytes
0	15	52	10	5	299
1	30	24	10	2	299
2	60	11	10	1	299

scenarios where traditional physical-layer advantages of higher numerologies may be offset by increased resource contention.

III. SIMULATION SETUP

The MoReV2X simulation tool [18], based on ns-3, is utilized to model vehicle mobility, propagation, and multiple access, focusing on sub-6 GHz NR-V2X communications (FR1). The simulation employs Mode 2 sidelink for direct Vehicle-to-Vehicle (V2V) communication, integrating DS and SPS mechanisms, alongside Wireless Blind Spot (WBS).

We simulate a highway scenario with a 5000 m stretch, featuring three lanes in each direction, with vehicles traveling at a speed of 70 km/h. The minimum safe headway between vehicles is set to 23 m, resulting in a maximum vehicle density of 154 veh/km (as per [6]). The average vehicle density is 140 veh/km.

Transmit power is 23 dBm, and the Received Signal Strength Indicator (RSSI) threshold is set to −92.3 dBm. The initial Reference Signal Receive Power (RSRP) threshold is −120.27 dBm, with the minimum fraction of SCs required in the selection list set to 20 %. Path loss and shadowing models follow [19], while Block-Error Rate (BLER) curves from [20] model fast-fading impairments.

Two different scenarios are simulated based on varying mean Channel Busy Ratio (CBR): one with low channel load ($\mathbb{E}[CBR] = 0.5$) and another with high channel load ($\mathbb{E}[CBR] = 0.95$). For the low channel load, the Medium Access Control (MAC) sub-layer operates with an RRI of 100 ms, and periodic traffic has a message generation interval of 100 ms. In the high channel load scenario, both the RRI and message generation time are set to 20 ms. In all scenarios we use only periodic network traffic.

NR-V2X radios operate on a 10 MHz channel within the 5.9 GHz ITS band. To maintain a consistent transport block size of 299 Byte with an Modulation and Coding Scheme (MCS) 13 configuration (16-QAM, 490/1024 code rate) across different numerologies, each SC uses 10 Resource Blocks (RBs), limiting the available channel configurations (according to [17]) as shown in Table I. Each slot includes one SC, resulting in 500 SCs for $\mu = 0$, and 400 SCs for $\mu = 1$ and $\mu = 2$ per RRI (as illustrated in Figure 1).

The OFDM numerology is configured with $\mu = 0, 1, 2$, a SCS of 15, 30 and 60 kHz, and slot durations of 1, 0.5 and 0.25 ms, respectively.

The Signal-to-Noise-plus-Interference Ratio (SNIR) value determines the BLER for successful message reception [20]. It should be noted that different BLER curves are associated with different numerologies, which will result in varying performance outcomes. System parameters are summarized in Table II.

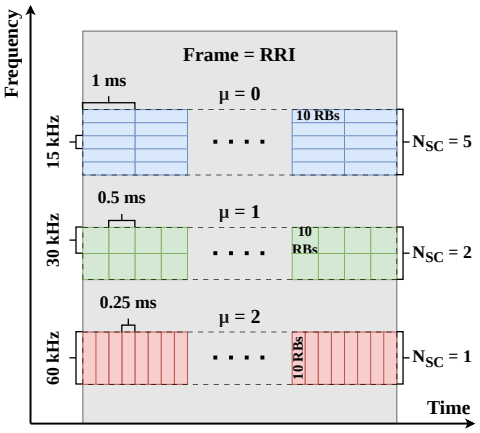

Figure 1. Example of sidelink channel configuration with different numerologies that guarantees a consistent transport block size with a channel bandwidth of 10 MHz

Table II
NUMERICAL VALUES OF MAIN SYSTEM PARAMETERS.

Parameter	**Values**
Highway length, L	5000 m
Vehicle density, ρ	140 veh/km
Maximal vehicle density, ρ_{max}	154 veh/km
Number of lanes	6
Vehicle speed	70 km/h
RRI	100 and 20 ms
Mean Channel Busy Ratio, $E[CBR]$	0.5 and 0.95
Message generation time, T_{gen}	100 ms
Channel bandwidth, BW	10 MHz
OFDM numerology, μ	0, 1, 2
Sub-Carrier Spacing, B_{sc}	15, 30 and 60 kHz
Time slot duration, T_s	1, 0.5 and 0.25 ms
MCS	MCS-13
Modulation	16 QAM
Code rate	0.4875
# of RBs per Sub-Channel, N_{RB}	10
# of Sub-Channels per time slot, N_{SC}	5, 2, 1
Transport Block Size, S_{TBS}	299 bytes
Transmission power	23 dBm
RSRP threshold	−120.07 dBm
Noise figure	9 dB
Margin for idle/busy channel assessment	3 dB
SC re-selection back-off factor	3 dB
Probability of persistence, P	[0; 0.995]
Reselection Counter, $\overline{RC}$	1

IV. PERFORMANCE EVALUATION

The simulations span the full persistence performance range defined for Geometric Semi-Persistent Scheduling (G-SPS) in [6], where persistence is categorized into four classes: DS, weak persistence, moderate persistence corresponding to the standardized SPS, and strong persistence. As in [6], η denotes the mean number of consecutive transmissions on the same SC, reflecting the persistence class, and is defined as

$$\eta = \frac{\overline{RC}}{1-P} = \frac{1}{1-P}. \tag{1}$$

In distance-based plots, DS corresponds to $\eta = 1$, while weak, moderate, and strong persistence correspond to $\eta = 2$, $\eta = 20$, and $\eta = 200$, respectively. In η-based plots, persistence classes are indicated as DS (black markers), weak (green zone), moderate (yellow zone), and strong (red zone).

A. Key performance metrics

1) Packet reception ratio (PRR): For broadcast communications, the PRR (Type 1 in [19]) measures the ratio of successfully received packets within a given distance range $[a, b]$.

For packet j, the instantaneous PRR is defined as

$$\text{PRR}_j = \frac{O_j}{H_j}, \tag{2}$$

where O_j is the number of nodes that correctly decode packet j within $[a, b]$, and H_j is the total number of nodes located in $[a, b]$.

Over M transmitted packets, the average PRR is

$$\text{PRR} = \frac{\sum_{j=1}^{M} O_j}{\sum_{j=1}^{M} H_j}. \tag{3}$$

2) Packet Inter-Reception (PIR): The PIR (also referred to as Peak AoI [7, 21]) is defined as the time interval between two consecutive successful receptions from the same transmitter.

Let $t_{ij}(k)$ denote the reception time of the k-th successfully received packet sent by node i to node j. The k-th PIR sample is

$$Y_{ij}(k) = t_{ij}(k) - t_{ij}(k-1). \tag{4}$$

The average PIR from node i to node j is

$$\mathbb{E}[\text{PIR}_{ij}] = \frac{1}{u_{ij}} \sum_{k=1}^{u_{ij}} Y_{ij}(k), \tag{5}$$

where u_{ij} is the number of successfully received packets.

The average PIR at node j is obtained as

$$\mathbb{E}[\text{PIR}_j] = \sum_{i \in \mathcal{N}_j} \frac{u_{ij}}{\sum_{k \in \mathcal{N}_j} u_{kj}} \mathbb{E}[\text{PIR}_{ij}]. \tag{6}$$

3) Collision Loss Ratio (CLR) and Propagation Loss Ratio (PLR): The Collision Loss Ratio (CLR) and Propagation Loss Ratio (PLR) quantify packet losses due to collisions and propagation impairments, respectively:

$$\text{CLR} = \frac{N_{\text{CL}}}{N_{\text{SR}} + N_{\text{CL}} + N_{\text{PL}}}, \tag{7}$$

$$\text{PLR} = \frac{N_{\text{PL}}}{N_{\text{SR}} + N_{\text{CL}} + N_{\text{PL}}}, \tag{8}$$

where N_{SR} is the number of successfully received packets, N_{CL} the number of packets lost due to collisions, and N_{PL} the number lost due to insufficient SNR.

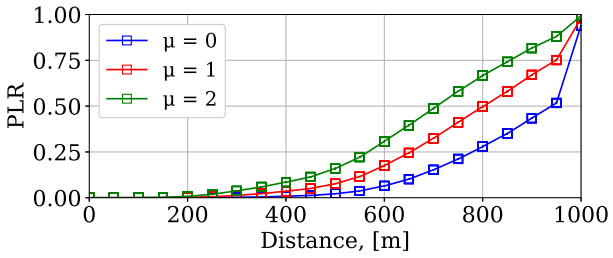

Figure 2. PLR as a function of transmitter–receiver distances for different numerologies. Note that PLR is independent of the mean CBR.

4) Age of Information (AoI): The AoI for updates sent by node i and received by node j is defined as

$$A_{ij}(t) = t - t_{ij}(k-1), \quad t \in [t_{ij}(k-1), t_{ij}(k)). \tag{9}$$

The time-average AoI is given by

$$\mathbb{E}[\text{AoI}_{ij}] = \lim_{T \to \infty} \frac{1}{T} \int_0^T A_{ij}(t)\, dt \approx \frac{\sum_{k=1}^{u_{ij}} \frac{1}{2} Y_{ij}^2(k)}{\sum_{k=1}^{u_{ij}} Y_{ij}(k)}. \tag{10}$$

The average AoI and PIR are related by

$$\mathbb{E}[\text{AoI}] = \frac{\mathbb{E}[\text{PIR}^2]}{2\,\mathbb{E}[\text{PIR}]}. \tag{11}$$

B. Results analysis

This section analyzes 5G NR-V2X sidelink communication performance for the scenarios introduced in Section III, using the metrics defined in Section IV-A and varying numerology-persistence coupling settings.

Figure 2 shows the PLR as a function of the transmitter–receiver distance for different numerologies. Note that the PLR is independent of the mean CBR and of the persistence configuration. However, increasing the numerology leads to higher PLR values with distance more then 250 m due to the degradation of BLER performance and the increased physical-layer complexity associated with higher numerologies.

Figures 3 and 4 show the PRR as a function of the persistence parameter η for different numerologies. Two transmitter–receiver distance ranges are considered: (a) 0–250 m, where attenuation effects are negligible, and (b) 250–500 m, where attenuation becomes significant while reliable inter-vehicle communication remains critical. For each range, results are reported under both low ($\mathbb{E}[\text{CBR}] = 0.5$) and high ($\mathbb{E}[\text{CBR}] = 0.95$) channel loading. The PRR differences across numerologies are marginal in Figure 3a. In contrast, Figures 3b, 4a and 4b reveal a clear separation between numerology $\mu = 0$ and numerologies $\mu = 1$ and $\mu = 2$, which exhibit nearly identical behavior. Under low channel loading, this separation is primarily driven by propagation losses. Under high channel loading, it arises from differences in the size of the resource pool available for allocation, reservation, and transmission within a frame. For $\mu = 0$, and assuming identical transport block sizes, the channel configuration enables a larger number of usable resources, resulting in fewer collisions and higher PRR. This behavior is clearly illustrated in Figures 5 and 6,

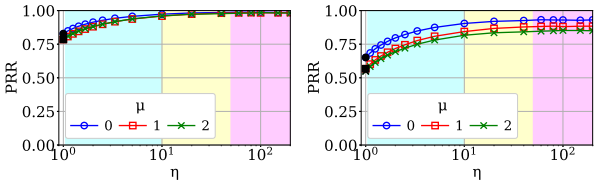

(a) 0–250 m (b) 250–500 m

Figure 3. PRR as a function of η for $\mathbb{E}[\mathrm{CBR}] = 0.5$ and different numerologies: (a) transmitter–receiver distances of 0–250 m, and (b) 250–500 m.

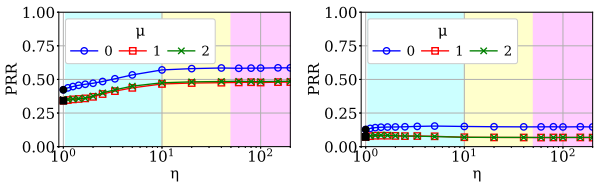

(a) 0–250 m (b) 250–500 m

Figure 4. PRR as a function of η for $\mathbb{E}[\mathrm{CBR}] = 0.95$ and different numerologies: (a) transmitter–receiver distances of 0–250 m, and (b) 250–500 m.

which show the CLR as a function of η. The number of collisions observed with numerology $\mu = 0$ is less than that observed with numerologies $\mu = 1$ and $\mu = 2$.

Timeliness metrics such as PIR and AoI, which are critical for autonomous vehicle safety applications, are highly sensitive to both the frequency and duration of collision events. Figures 7 and 8 analyze PIR performance as a function of persistence, following an approach analogous to that used for PRR and CLR. In Figure 7 PIR is largely independent of the numerology, since under low channel loading the available resources are sufficient to accommodate collisions without significantly affecting

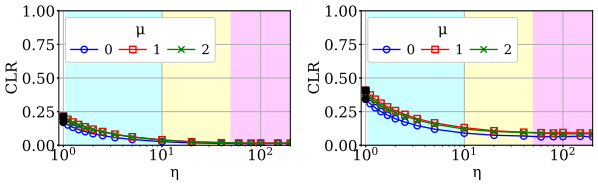

(a) 0–250 m (b) 250–500 m

Figure 5. CLR as a function of η for $\mathbb{E}[\mathrm{CBR}] = 0.5$ and different numerologies: (a) transmitter–receiver distances of 0–250 m, and (b) 250–500 m.

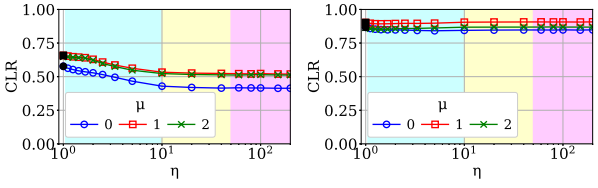

(a) 0–250 m (b) 250–500 m

Figure 6. CLR as a function of η for $\mathbb{E}[\mathrm{CBR}] = 0.95$ and different numerologies: (a) transmitter–receiver distances of 0–250 m, and (b) 250–500 m.

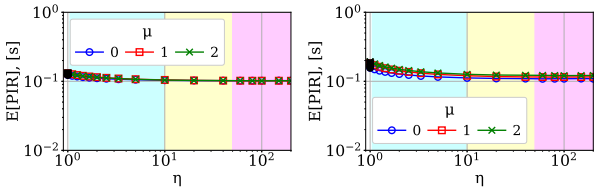

(a) 0–250 m (b) 250–500 m

Figure 7. PIR as a function of η for $\mathbb{E}[\mathrm{CBR}] = 0.5$ and different numerologies: (a) transmitter–receiver distances of 0–250 m, and (b) 250–500 m.

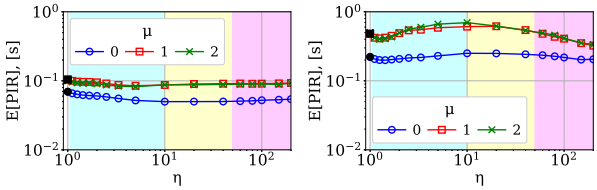

(a) 0–250 m (b) 250–500 m

Figure 8. PIR as a function of η for $\mathbb{E}[\mathrm{CBR}] = 0.95$ and different numerologies: (a) transmitter–receiver distances of 0–250 m, and (b) 250–500 m.

update regularity. In contrast, under high channel loading (Figure 8), a clear advantage of numerology $\mu = 0$ emerges. This behavior is driven by increased resource contention and the correspondingly higher CLR, which disproportionately affect numerologies with smaller effective resource pools.

However, as shown in [6], PIR is only weakly sensitive to collision duration and is predominantly determined by the selected persistence level. Figures 9 and 10 exhibit trends similar to those observed for PIR with respect to performance differences across numerologies. Under high channel load, numerology $\mu = 0$ again outperforms the other configurations. Notably, the AoI performance as a function of persistence

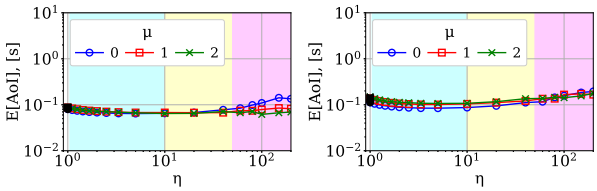

(a) 0–250 m (b) 250–500 m

Figure 9. AoI as a function of η for $\mathbb{E}[\mathrm{CBR}] = 0.5$ and different numerologies: (a) transmitter–receiver distances of 0–250 m, and (b) 250–500 m.

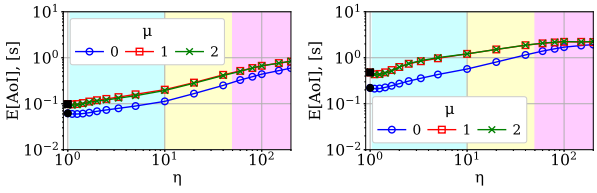

(a) 0–250 m (b) 250–500 m

Figure 10. AoI as a function of η for $\mathbb{E}[\mathrm{CBR}] = 0.95$ and different numerologies: (a) transmitter–receiver distances of 0–250 m, and (b) 250–500 m.

exhibits non-monotonic behavior for all numerology values, whereas this effect had previously been reported only for $\mu = 0$ [6, 7]. In Figure 9, under low channel loading, the minimum mean AoI is achieved with weak or moderate persistence, corresponding to standard SPS configurations. Under high channel loading, the minimum mean AoI is achieved with weak persistence or DS, which is significantly simpler to implement in certain applications than any SPS-based configuration.

V. Conclusions

This work revisits numerology-persistence coupling selection in 5G NR-V2X sidelink and analyzes its impact beyond physical-layer aspects. Although scalable numerology is designed to accommodate diverse frequency bands and mobility regimes, sidelink configuration should be assessed within a cross-layer framework.

Higher numerologies reduce slot duration and improve Doppler robustness, which is beneficial for mmWave and extreme mobility. However, in sub-6 GHz deployments with limited bandwidth and high channel load, these gains do not necessarily translate into better end-to-end performance. Increased propagation losses and reduced MAC-layer resource availability constrain scheduling and reservation efficiency.

As channel load increases, the resulting MAC-layer constraints can offset the physical-layer benefits of higher numerologies, leading to increased collision activity, longer disconnection periods, and degraded timeliness. Conversely, lower numerologies benefit from larger effective resource pools and improved spectral efficiency, which enhance robustness under congestion despite their longer nominal transmission intervals.

For the evaluated scenario with a 10 MHz channel bandwidth and a fixed transport block size of 299 Byte, numerology $\mu = 0$ consistently achieved the most favorable balance across reliability, timeliness, and connectivity metrics, particularly when combined with dynamic scheduling or weak persistence. These findings do not challenge the motivation behind scalable numerology in 5G NR, but rather complement it by highlighting the importance of jointly considering physical-layer and MAC-layer effects when configuring NR-V2X sidelink for safety-critical vehicular applications.

Acknowledgment

This work was partially funded by Sapienza University of Rome under the “Progetti per Avvio alla Ricerca – Tipo 2” program (2025) for the project “Advancing 5G Vehicular Communication for Real-Time Awareness and VRU Protection” (prot. AR225199B968B6C6), partially supported by the Italian Ministry of University and Research under the PRIN program (project code 20223Y85JN), project “LOREN – LOw-delay congestion control for REal-time applications over the iNternet” (CUP: B53D23002200006), and partly supported by "Country to City Bridge 2 - C2CBridge 2” project of the German Center for Future Mobility, funded by the German Federal Ministry for Digital and Transport.

References

[1] 3GPP, “5G; NR; NR and NG-RAN Overall Description; Stage 2 (Release 19),” 3GPP, TS 38.000 V19.1.0, Dec. 2025.

[2] 3GPP, “5G; NR; Physical channels and modulation (Release 19),” 3GPP, TS 38.000 V19.2.0, Dec. 2025.

[3] M. H. C. Garcia et al., “A tutorial on 5G NR V2X communications,” *IEEE Communications Surveys & Tutorials*, vol. 23, no. 3, pp. 1972–2026, 2021.

[4] S. Khabaz, K. O. Boulila, T. M. Trang Nguyen, G. Pujolle, M. El Aoun, and P. B. Velloso, “A Comprehensive Study of the Impact of 5G Numerologies on V2X Communications,” in *2022 13th International Conference on Network of the Future (NoF)*, 2022, pp. 1–9.

[5] J. Flores de Valgas, J. F. Monserrat, and H. Arslan, “Flexible Numerology in 5G NR: Interference Quantification and Proper Selection Depending on the Scenario,” *Mobile Information Systems*, vol. 2021, no. 1, p. 6 651 326, 2021.

[6] A. Rolich, M. Yildiz, I. Turcanu, A. Vinel, and A. Baiocchi, “Rethinking Persistent Scheduling in 5G New Radio Vehicle-to-Everything Sidelink Communications,” *IEEE Access*, vol. 13, pp. 164 065–164 083, 2025.

[7] A. Rolich, I. Turcanu, A. Vinel, and A. Baiocchi, “Understanding the impact of persistence and propagation on the Age of Information of broadcast traffic in 5G NR-V2X sidelink communications,” *Computer Networks*, vol. 248, 2024.

[8] C. Campolo, A. Molinaro, F. Romeo, A. Bazzi, and A. O. Berthet, “5G NR V2X: On the Impact of a Flexible Numerology on the Autonomous Sidelink Mode,” in *2019 IEEE 2nd 5G World Forum (5GWF)*, 2019, pp. 102–107.

[9] Z. Ali, S. Lagén, and L. Giupponi, “On the impact of numerology in NR V2X Mode 2 with sensing and random resource selection,” in *2021 IEEE Vehicular Networking Conference (VNC)*, 2021, pp. 151–157.

[10] D. Segura, E. J. Khatib, J. Munilla, and R. Barco, “5G Numerologies Assessment for URLLC in Industrial Communications,” *Sensors*, vol. 21, no. 7, 2021.

[11] A. Hossain and N. Ansari, “5G Multi-Band Numerology-Based TDD RAN Slicing for Throughput and Latency Sensitive Services,” *IEEE Transactions on Mobile Computing*, vol. 22, no. 3, pp. 1263–1274, 2023.

[12] N. Patriciello, S. Lagen, L. Giupponi, and B. Bojovic, “5G New Radio Numerologies and their Impact on the End-To-End Latency,” in *2018 IEEE 23rd International Workshop on Computer Aided Modeling and Design of Communication Links and Networks (CAMAD)*, 2018, pp. 1–6.

[13] D. Wang, O. Saraci, R. R. Sattiraju, Q. Zhou, and H. D. Schotten, “Effect of Variable Physical Numerologies on Link-Level Performance of 5G NR V2X,” in *2022 IEEE 8th International Conference on Computer and Communications (ICCC)*, 2022, pp. 291–296.

[14] D. Wang, P. B. Mohite, Q. Zhou, A. Qiu, and H. D. Schotten, “Evaluating the Impact of Numerology and Retransmission on 5G NR V2X Communication at A System-Level Simulation,” in *2023 IEEE Conference on Standards for Communications and Networking (CSCN)*, 2023, pp. 59–65.

[15] T. Soni, A. R. Ali, K. Ganesan, and M. Schellmann, “Adaptive numerology — A solution to address the demanding QoS in 5G-V2X,” in *2018 IEEE Wireless Communications and Networking Conference (WCNC)*, 2018, pp. 1–6.

[16] A. Rolich, M. Yildiz, I. Turcanu, A. Vinel, and A. Baiocchi, “On the Trade-off Between AoI Performance and Resource Reuse Efficiency in 5G NR V2X Sidelink,” in *2025 IEEE Vehicular Networking Conference (VNC)*, 2025, pp. 1–8.

[17] 3GPP, “5G; NR; User Equipment (UE) radio transmission and reception; Part 1: Range 1 Standalone (Release 19),” 3GPP, TS 38.101-1 V19.4.0, Dec. 2025.

[18] L. Lusvarghi and M. L. Merani, “MoReV2X - A New Radio Vehicular Communication Module for ns-3,” in *2021 IEEE 94th Vehicular Technology Conference (VTC2021-Fall)*, 2021, pp. 1–7.

[19] 3GPP, “Study on evaluation methodology of new Vehicle-to-Everything (V2X) use cases for LTE and NR;(Release 15),” 3GPP, TR 37.885 V15.3.0, Jun. 2019.

[20] L. Lusvarghi, B. Coll-Perales, J. Gozalvez, and M. L. Merani, “Link Level Analysis of NR V2X Sidelink Communications,” *IEEE Internet of Things Journal*, vol. 11, no. 17, pp. 28 385–28 397, 2024.

[21] A. Rolich, I. Turcanu, A. Vinel, and A. Baiocchi, “Impact of Persistence on the Age of Information in 5G NR-V2X Sidelink Communications,” in *21st Mediterranean Communication and Computer Networking Conference (MedComNet)*, Ponza Island, Italy: IEEE, Jun. 2023, pp. 15–24.